Supporting information for: Dynamic organization of soft nanoparticles during adsorption and surface compression at fluid-fluid interfaces

Axel Huerre,[†,‡] Fernando Cacho-Nerin,[¶,‡] Vincent Poulichet,[†,§] Christiana E. Udoh,[†] Marco De Corato,[†] and Valeria Garbin[*,†]

†*Department of Chemical Engineering, Imperial College London, London SW7 2AZ, United Kingdom*

‡*A. H. and F. C.-N. contributed equally*

¶*Diamond Light Source, Harwell Science and Innovation Campus, Didcot OX11 ODE, United Kingdom*

§*Current address: Complex Fluids Group, School of Chemical Engineering, UNSW Sydney, Sydney, Australia*

E-mail: v.garbin@imperial.ac.uk

Validation of X-ray contrast.

An X-ray sensitive diode was positioned downstream of the drop at approximatley 200 mm and used as a single-element detector. The oil drop was incubated for 15 minutes in the nanoparticle suspension, and the suspension was then replaced with water (10 mL of water at 10 mL/min). The droplet was then raster-scanned across the beam at 50 μm intervals

through the droplet, with an exposure time of 3 s at each point. The resulting image (see Fig. 1) is a radiograph of the drop. The drop shape can be clearly seen and intenisty measurement performed. We first measured from the picture the background intensity I_0^w that can be written as

$$I_0^w = I_0 e^{-\mu_w l} = 4 \cdot 10^6 \tag{1}$$

where I_0 is the beam incoming intensity, μ_w=0.183926 mm^{-1} the attenuation factor of water at 14 keV, and l=5mm the distance travelled in water. The beam nominal intensity is thus $I_0 = 10 \cdot 10^6$. In the central region of the droplet, the beam travels in the water over a distance $l - 2R$ and through the oil over a distance $2R$, where $2R = 1.8$mm is the droplet diameter. The intensity in this region writes:

$$I^o = I_0 e^{-\mu_o 2R - \mu_w (l-2R)} = 2.8 \cdot 10^6 \tag{2}$$

We deduce from this calculation the attenuation factor of OFPA in our conditions, μ_o=0.38 mm^{-1}. The difference in optical density found between OFPA and water in our conditions ensures that, when they illuminate the interface at a shallow angle, the X-rays will be reflected off the droplet surface instead of bent into it. Furthermore, in transmission geometry, the 4.5-nm nanoparticle film is effectively transparent to X-rays and does not contribute to the contrast in the image. As expected, the steel needle is completely opaque.

GISAXS data pre-processing.

Because the liquid cell was repositioned with respect to the x-ray beam after each incremental withdrawal, the beam illuminated the droplet at a slightly different azimuthal angle in each frame, and the orientation of the reflected beam on the detector changed accordingly. Thus, in order to analyze the data in a consistent way, the frames from each exposure were aligned by transforming the images into polar coordinates using the centre position from the SAXS

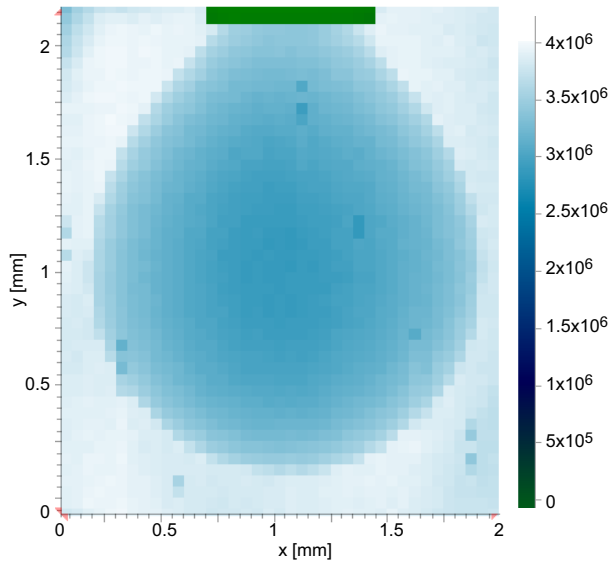


Figure 1: X-ray transmission image of the pendant drop acquired with a diode sensor with a pixel resolution of 50 μm.

calibrant as the origin for the transformation (see Figure 2 (i)). A line cut was then taken at a fixed radius from the beam center and a Lorentzian peak was fitted to the reflected beam, to yield the exact azimuthal angle of the beam on the droplet surface (Figure 2 (ii)). Using this angle, we then remapped the raw detector image into GISAXS coordinates, i.e. into in-plane and out-of-plane components (Figure 2 (iii)). The in-plane profile $I(q_{||})$ at $q_{\perp}$= =0.349 nm^{-1} was then extracted and used for the analysis (Figure 2 (iv)). These preprocessing operations were carried out with the freely available Data Analysis WorkbeNch.[1]

Error quantification.

Figure 3 shows $q_{||}$ as a function of time for the adsorption experiment. We notice that except for the first point, error bars represent less than 1 % variations. However, the propagation of errors from inverse to direct space is not straightforward. In order to provide goodness-of-fit estimates, the fitting routine assumes that each parameter follows a normal distribution allowing the extraction of the peak position and a standard deviation. The interparticle distance is written as $d = 4\pi/(\sqrt{3}q_{||})$. If we assume a normal distribution for the peak

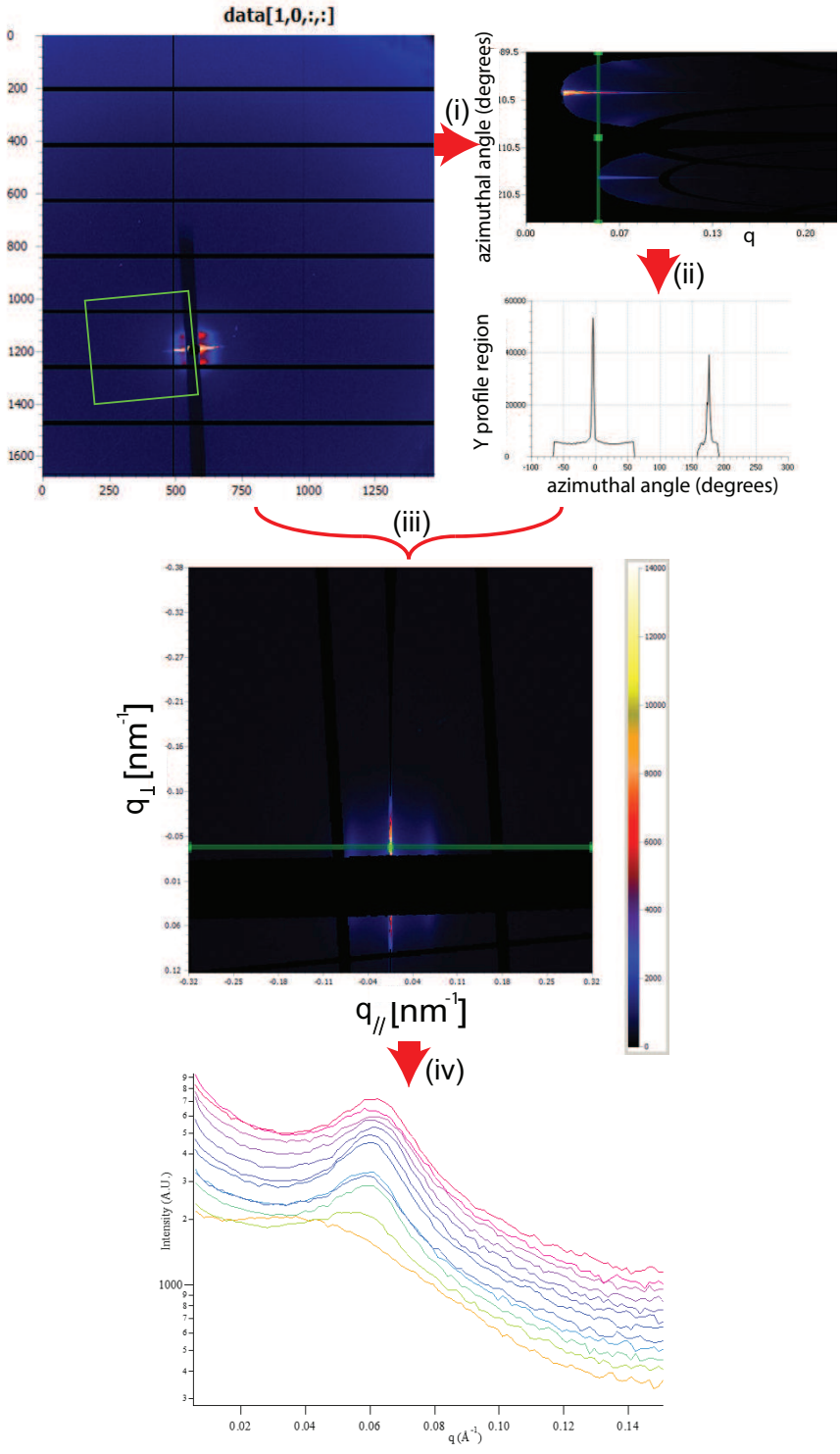


Figure 2: Workflow diagram of the pre-processing method.

position, the distribution of d is then bimodal. Consequently, the first and higher-order moments do not exist and we cannot ascribe error bars for the distances.

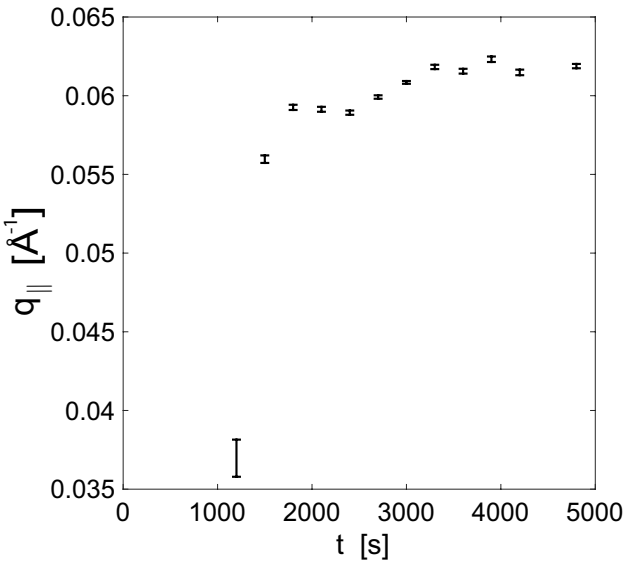


Figure 3: $q_{\parallel}$ as a function of time for the adsorption experiment. Except for the first point, error bars represent less than 1 % variations.

Simulations: interaction potential.

Figure 4 shows the evolution of the interaction potential (see Eq. (1) in the main text) as a function of the interparticle distance. The parameters used in the plot are $\sigma = 5.5$ chains/nm^2, L=3.5 nm, $a_{\text{core}} = 2.3$ nm which comes from the experimental values after adsorption. The interaction is force resulting from this potential is always repulsive and increases steeply when reaching small distances.

References

(1) Filik, J.; Ashton, A. W.; Chang, P. C. Y.; Chater, P. A.; Day, S. J.; Drakopoulos, M.; Gerring, M. W.; Hart, M. L.; Magdysyuk, O. V.; Michalik, S.; Smith, A.; Tang, C. C.; Terrill, N. J.; Wharmby, M. T.; Wilhelm, H. Processing two-dimensional X-ray diffraction

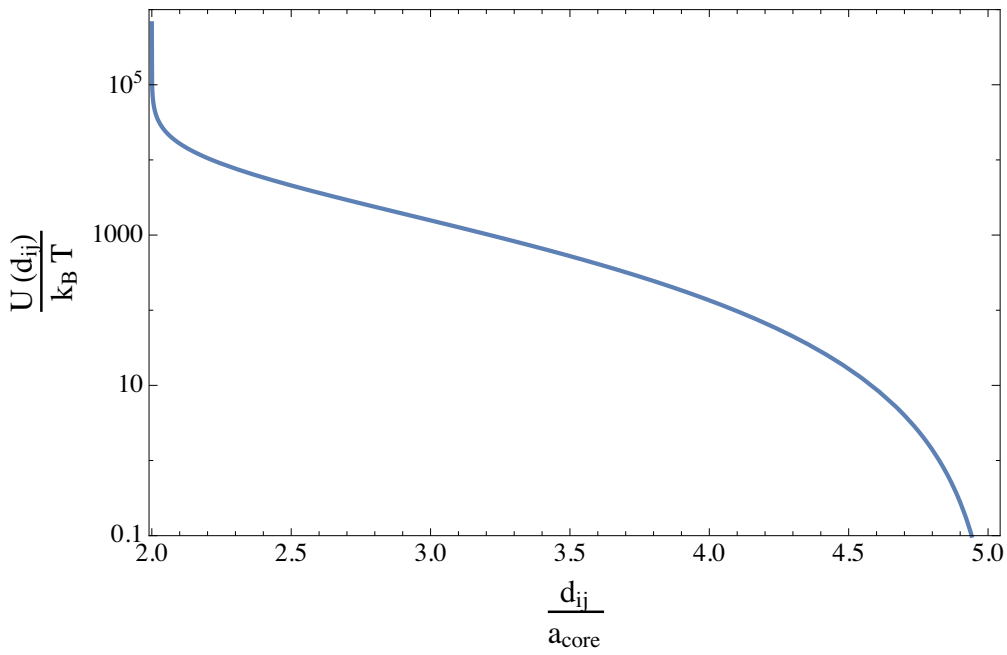


Figure 4: Log-lin plot of the normalized interaction potential U_{ij}/k_BT as a function of the reduced interparticle center-to-center distance d_{ij}/a_{core} for distances smaller that $2a_{\text{core}}+2L$.

and small-angle scattering data in *DAWN 2*. *Journal of Applied Crystallography* **2017**, *50*, 959–966.